CORRECTED 31 MAY 2022; SEE FULL TEXT

GENETICS

ETS1 acts as a regulator of human healthy aging via decreasing ribosomal activity

Fu-Hui Xiao[1,2]†, Qin Yu[1,2]†, Zhi-Li Deng[3,4,5]†, Ke Yang[2,6,7], Yunshuang Ye[2,6,7], Ming-Xia Ge[1,2,6,8,9], Dongjing Yan[10], Hao-Tian Wang[1,2,6,8,9], Xiao-Qiong Chen[1], Li-Qin Yang[1], Bin-Yu Yang[1], Rong Lin[11], Wen Zhang[10], Xing-Li Yang[1], Lei Dong[1], Yonghan He[1], Jumin Zhou[2,7,9], Wang-Wei Cai[10]*, Ji Li[3,4,5]*, Qing-Peng Kong[1,2,8,9]*

Adaptation to reduced energy production during aging is a fundamental issue for maintaining healthspan or prolonging life span. Currently, however, the underlying mechanism in long-lived people remains poorly understood. Here, we analyzed transcriptomes of 185 long-lived individuals (LLIs) and 86 spouses of their children from two independent Chinese longevity cohorts and found that the ribosome pathway was significantly down-regulated in LLIs. We found that the down-regulation is likely controlled by *ETS1* (ETS proto-oncogene 1), a transcription factor down-regulated in LLIs and positively coexpressed with most ribosomal protein genes (RPGs). Functional assays showed that ETS1 can bind to RPG promoters, while *ETS1* knockdown reduces RPG expression and alleviates cellular senescence in human dermal fibroblast (HDF) and embryonic lung fibroblast (IMR-90) cells. As protein synthesis/turnover in ribosomes is an energy-intensive cellular process, the decline in ribosomal biogenesis governed by *ETS1* in certain female LLIs may serve as an alternative mechanism to achieve energy-saving and healthy aging.

INTRODUCTION

Impaired cellular energy production due to dysfunction of mitochondria represents a crucial driver of aging and age-related disorders (*1*, *2*). Therefore, how to address this energy crisis plays an important role in determining healthy aging and longevity in aged people. Longevity pathways (e.g., mammalian target of rapamycin) and interventions (e.g., calorie restriction) rely on the improvement of mitochondrial activity (*3*, *4*). Notably, aging is also thought to be caused by hyperfunction, whereby the continued activity of developmental programs in late life leads to pathological issues and eventually to death (*5*, *6*). However, the slowdown or shutoff of biological processes in late life to avoid energy overconsumption and facilitate healthy human aging and longevity has yet to be explored.

As a paradigm of successful human aging, long-lived individuals (LLIs) achieve extreme old age without developing serious age-related diseases (e.g., cardiovascular disease, neurodegenerative disorders, and cancer) (*7*, *8*). Gene expression is thought to have a close association with the activity of processes involved in healthy aging and longevity in LLIs (*9*, *10*). Here, to find the processes displaying reduced biological activities in long-lived people, we obtained and analyzed the transcriptomes of peripheral white blood cells from 185 female LLIs and 86 gender-matched spouses of LLI children (F1SPs) from two independent Chinese longevity cohorts. Results showed that genes related to the ribosome pathway, especially ribosomal protein genes (RPGs), were significantly down-regulated in the LLIs. We also found that most of the RPGs were positively coexpressed with the *ETS1* gene, which was down-regulated in LLIs. This gene encodes a transcription factor (TF) that binds to RPG promoters, and its down-regulation leads to the reduced RPG expression. Furthermore, knockdown of *ETS1* alleviated cellular senescence and suppressed RPG transcription in human dermal fibroblast (HDF) and human embryonic lung fibroblast (IMR-90) cells. Thus, these findings reveal that decreased ribosome biogenesis caused, at least in part, by the down-regulation of *ETS1* exists in certain female LLIs and may contribute to healthy aging and life span extension in long-lived people.

[1]State Key Laboratory of Genetic Resources and Evolution/Key Laboratory of Healthy Aging Research of Yunnan Province, Kunming Institute of Zoology, Chinese Academy of Sciences, Kunming 650201, China. [2]Kunming Key Laboratory of Healthy Aging Study, Kunming 650201, China. [3]Department of Dermatology/National Clinical Research Center for Geriatric Disorders, Xiangya Hospital, Central South University, Changsha 410000, China. [4]Hunan Key Laboratory of Aging Biology, Xiangya Hospital, Central South University, Changsha 410000, China. [5]Department of Dermatology, Second affiliated Hospital of Xinjiang Medical University, Urumqi 830000, China. [6]Kunming College of Life Science, University of Chinese Academy of Sciences, Beijing 100049, China. [7]Key Laboratory of Animal Models and Human Disease Mechanisms of the Chinese Academy of Sciences, Kunming Institute of Zoology, Kunming 650223, China. [8]CAS Center for Excellence in Animal Evolution and Genetics, Chinese Academy of Sciences, Kunming 650223, China. [9]KIZ/CUHK Joint Laboratory of Bioresources and Molecular Research in Common Diseases, Kunming 650223, China. [10]Department of Biochemistry and Molecular Biology, Hainan Medical College, Haikou 571199, China. [11]Department of Biology, Hainan Medical College, Haikou 571199, China.
*Corresponding author. Email: kongqp@mail.kiz.ac.cn (Q.-P. K.); liji_xy@csu.edu.cn (J. L.); caiww591020@163.com (W.-W. C.)
†These authors contributed equally to this work.

RESULTS

RNA sequencing of LLIs and F1SPs from two independent longevity cohorts

We selected a total of 271 female individuals, including 185 LLIs (age, 98.9 ± 3.8 years; means ± SD) and 86 F1SPs (age, 57.4 ± 9.0 years; means ± SD) from two independent longevity cohorts from the Lingshui (LS) and Lingao (LG) prefectures, Hainan Province, China (viz. LS and LG cohorts, respectively) (fig. S1). Among them, 135 individuals (80 LLIs and 55 F1SPs) from the LS cohort were used in the discovery stage, and 136 individuals (105 LLIs and 31 F1SPs) from the LG cohort were used in the replication stage. The blood cell composition [i.e., lymphocytes (Lymph), neutrophils (Neu), and monocytes (Mon)] of the LS samples was successfully obtained, with the proportion of monocytes showing a difference between LLIs and F1SPs (fig. S2, A and B). Transcriptomes of peripheral white blood cells were generated on the Illumina HiSeq platform (table S1). For

each cohort, gene-level read counts were calculated to assess gene expression levels, and protein-coding genes with at least 10 reads across all samples were used for subsequent analyses.

Identifying the down-regulated ribosome pathway in discovery cohort LLIs

In the first stage, we analyzed the transcriptome data of samples from the LS discovery cohort, which contained 13,537 protein-coding genes. Using a *P* value cutoff of <0.05 (*9*), we identified a total of 3487 differentially expressed genes (DEGs) between LLI and F1SP groups using the DESeq2 package (*11*), with consideration of the effects of library type and cell composition (Fig. 1A). Among the 3487 DEGs, 2905 were also identified in the LLIs using multiple linear regression combined with cell composition variables (see Materials and Methods). In addition, we used regression analysis to quantify the associations between age and gene expression in F1SP samples. Results showed that most (89.2%, 2590 of 2905) DEGs displayed no significant associations between expression and age in the middle-aged samples (i.e., F1SPs) ($P > 0.05$). Of these DEGs, 1411 were up-regulated, and 1179 were down-regulated in LLIs (Fig. 1, A and B). The median $\log_2$-transformed expression fold changes of the up- and down-regulated DEGs were 0.18 and −0.21, respectively (Fig. 1C).

To explore the functional pathways of the DEGs in healthy human aging and longevity, we performed enrichment analysis. Kyoto Encyclopedia of Genes and Genomes (KEGG) pathway analysis revealed that the up-regulated genes in LLIs were most significantly enriched in the lysosome pathway (Fig. 1D), echoing the findings of enhanced autophagy-lysosomal activity in our previous study (*9*). Unexpectedly, however, the down-regulated genes in the LS cohort were highly overrepresented in the ribosome pathway (hsa03010), the significance of which was far greater than that of the lysosomal signaling pathway (Fig. 1D). In addition, we found that the ribosome pathway is still highly enriched [Benjamini-Hochberg (BH)–corrected $P = 1.57 \times 10^{-33}$] among the 835 down-regulated genes identified under a stringent threshold of BH-adjusted $P < 0.05$ (fig. S3A).

The down-regulated genes in the ribosome pathway mainly are RPGs, which encode proteins constituting the small and large subunits of ribosome. We next investigated the LLI-specific transcription patterns of all RPGs collected from the RPG database (*12*). Among the collected 80 RPGs, 74 were detected by the RNA sequencing (RNA-seq) data, among which 66 (89.2%, 66 of 74) were significantly down-regulated in LLIs (Fig. 1E and table S2). The other eight RPGs also exhibited a decrease in expression in the LLIs, although it is statistically insignificant. Of the above 66 RPGs, 59 displayed no expression changes, and 7 were significantly reduced with age in the F1SP samples, suggesting that the overall expression of RPGs is not markedly down-regulated in middle age (table S2; fig. S4). Furthermore, we also explored the correlation of RPG expression with age using the whole blood gene expression data retrieved from the Genotype-Tissue Expression database (age, 20 to 79 years). Result showed that 54 of the 66 RPGs presented no correlation between their expression and age ($P > 0.05$) (fig. S5). Collectively, these findings suggest that the overall expression of RPGs is unlikely to be age dependent.

Ribosome biogenesis and protein synthesis are highly energy consuming cellular processes (*13*), the inhibition of which can extend the life span in diverse model organisms, including yeast, worms, and mice (*14*–*16*). Therefore, we focused on the down-regulated ribosome pathway, the most enriched signal in the LS cohort LLIs,

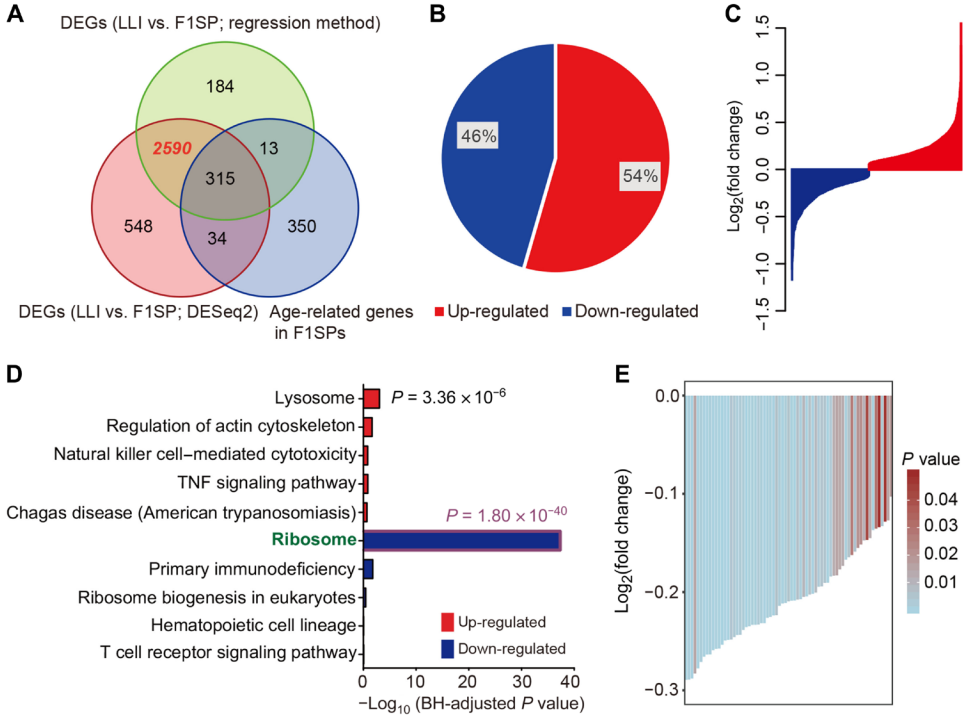

Fig. 1. DEGs between the LLI and F1SP groups from the discovery (i.e., LS) cohort. (**A**) Venn diagram for the identified DEGs. Number with red color represents the genes with expression differences between LLI and F1SP groups by methods of DESeq2 and regression analysis but without associations between their expression and age in F1SP samples. (**B**) Percentage of up- and down-regulated genes in LLIs. (**C**) Expression differences in LLI-specific DEGs. (**D**) KEGG pathway enrichment analysis for LLI-specific DEGs. TNF, tumor necrosis factor. (**E**) Expression differences for lowly expressed RPGs in LLI samples.

and investigated the key regulators that govern the LLI-specific RPG transcription profiles.

ETS1 as a contributor to down-regulated ribosomal genes in LS cohort LLIs

As ribosomal genes are always coexpressed (*17*), we searched for the TF-binding motifs enriched in the promoters of the down-regulated RPGs using the HOMER (Hypergeometric Optimization of Motif Enrichment) algorithm (*18*). Results showed that the top scoring TF motifs were involved in the ETS (E-twenty six) family, including Fli1 (friend leukemia integration 1) and ETS1 (Fig. 2A). Among these TFs, *ETS1* exhibited the most significant differential expression and was down-regulated in LLIs (Fig. 2B and table S3).

In addition, the heatmap plot showed that the LLIs with low *ETS1* expression also had down-regulated RPGs (Fig. 2C). Thus, we performed coexpression analysis to investigate the contribution of *ETS1* to the down-regulated ribosome pathway in LLIs. Among the 66 down-regulated RPGs, 53 (80.3%; 53 of 66) displayed significant positive associations between their expression and that of *ETS1* (Fig. 2D), suggesting that *ETS1* has a role in activating RPG expression.

Down-regulated ribosome pathway in replication cohort LLIs

To test whether the observations in the LS cohort could be repeated, we analyzed the transcriptome data from the LG cohort (consisting of 105 LLIs and 31 F1SPs), which included 12,755 protein-coding genes. Similarly, we identified 4065 genes with differential expression between the LLI and F1SP groups ($P < 0.05$), although no associations were found between their expression and age in F1SPs ($P > 0.05$) (Fig. 3A). In line with the above findings, the 2012 up-regulated genes were most enriched in the lysosome pathway, whereas the 2053 down-regulated genes were most enriched in the ribosome pathway (Fig. 3B). Similarly, the ribosome pathway is still significantly enriched (BH-corrected $P = 1.12 \times 10^{-51}$) on the basis of 1331 down-regulated genes that were identified using a more stringent threshold of BH-corrected $P < 0.05$ (fig. S3B). Further analysis revealed that 71 of the 80 RPGs in large and small ribosomal

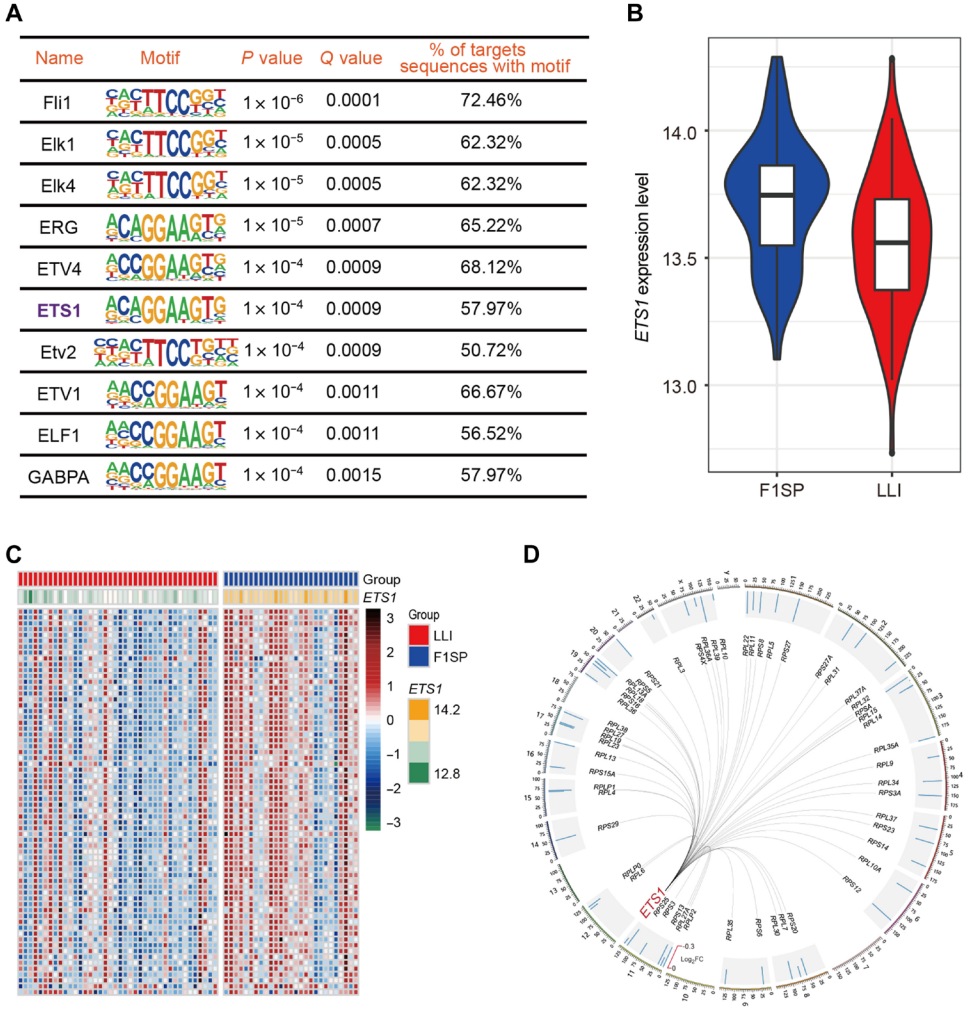

Fig. 2. Identification of key regulators governing LLI-specific RPG transcription patterns in discovery cohort. (**A**) TF-binding site motif analysis for down-regulated RPGs in LLIs. Elk1, ETS transcription factor Elk1; ERG, ETS transcription factor ERG; ELF1, E74 like ETS transcription factor 1; GABPA, GA binding protein transcription factor subunit alpha. (**B**) *ETS1* shows reduced expression in LLIs. (**C**) Heatmap plot shows that LLIs with low *ETS1* expression have reduced RPG expression. (**D**) *ETS1* is coexpressed with 53 down-regulated RPGs. FC, fold change.

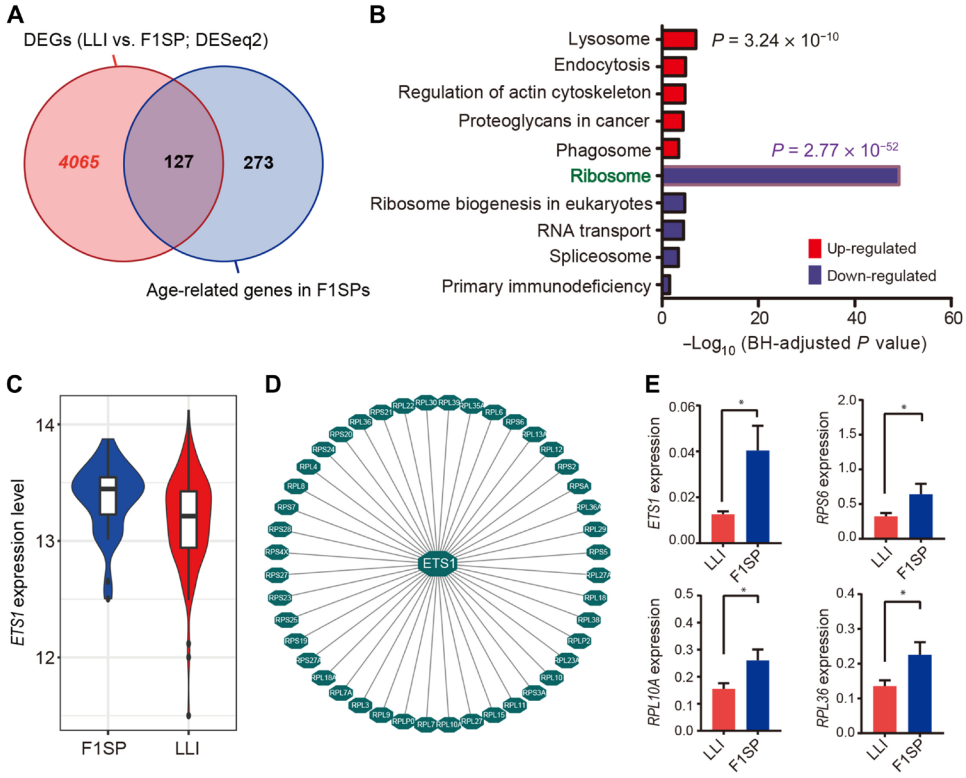

Fig. 3. DEG analysis in replication (i.e., LG) cohort. (**A**) Venn plot for DEGs in LLIs. (**B**) KEGG pathway enrichment for DEGs. (**C**) *ETS1* is down-regulated in LLIs. (**D**) *ETS1* is coexpressed with 44 down-regulated RPGs. (**E**) RT-qPCR validation for the expression of *ETS1* and three RPGs between LLIs and F1SPs. *$P < 0.05$.

subunits were down-regulated (figs. S4 and S6). Consistently, we found that *ETS1* was also significantly down-regulated in LLIs from the LG cohort (Fig. 3C). Furthermore, 44 of the 71 down-regulated RPGs were significantly and positively coexpressed with *ETS1* (Fig. 3D). In addition, we further combined and reanalyzed the transcriptome data of the two independent cohorts. Results showed that the 1756 LLI down-regulated genes (BH-adjusted $P < 0.05$) are mostly enriched in the ribosome pathway (BH-adjusted $P = 2.83 \times 10^{-52}$) and *ETS1* expression is significantly reduced in the LLIs (fig. S7). By investigating the gene expression changes of peripheral blood mononuclear cells from 172 health adults, 22 to 93 years of age (*19*), we found that 60 of the 80 RPGs show reduced expression levels in the healthy aging individuals, suggesting that the decreased expression of RPGs, at least a proportion of them, is more likely associated with healthy aging.

To validate the expression results generated by RNA-seq, we detected the expression level of *ETS1* by real-time quantitative polymerase chain reaction (RT-qPCR) and found that it exhibited low expression in LLIs compared to that in F1SPs (Fig. 3E). Similarly, three RPGs (i.e., *RPL36*, *RPL10A*, and *RPS6*) randomly detected by RT-qPCR were also down-regulated in the LLIs (Fig. 3E). These findings indicate that genes involved in the ribosome pathway tended to be down-regulated in LLIs in both the LS and LG cohorts and that *ETS1* likely contributed to the LLI-specific ribosomal transcription pattern.

ETS1 functions in RPG transcription regulation

To functionally test whether down-regulated *ETS1* expression decreases RPG expression, we first constructed *ETS1* knockdown 293T cells using short hairpin RNA (shRNA) expression plasmid (fig. S8A). Transcriptome analysis showed that the genes in the ribosome pathway were significantly down-regulated (Fig. 4, A and B, and fig. S8B), among which several randomly selected RPGs (e.g., *RPL3* and *RPS13*) were validated by RT-qPCR (fig. S8C). We also analyzed publicly available Ets1 (mouse homolog of *ETS1*) chromatin immunoprecipitation sequencing (ChIP-seq) data from primary mouse B cells to screen Ets1-binding sites across the genome (*20*) and found that the Ets1 target genes were significantly enriched in the ribosome pathway (fig. S9A). A similar result was also observed in human lymphoblastoid cells (GM12878) (fig. S9B). Thus, these findings indicate that the ETS1 likely plays a role in regulating RPG transcription.

ETS1 knockdown alleviates cell senescence and decreases RPG transcription

We then tested the effects of *ETS1* knockdown on HDF at passage 25 using small interfering RNA (siRNA) method (fig. S10A). Results showed that the reduced *ETS1* expression significantly decreased senescence-associated beta-galactosidase beta (SA-β-Gal) staining cell percentages and reduced *CDKN2A* (*p16*) and *CDKN1A* (*p21*) expression levels in the cell line (Fig. 4, C and D). SA-β-Gal is the most widely used indicator of cellular senescence (*21*); CDKN2A and CDKN1A are two important regulators that can initiate senescence (*22*). We also analyzed the expression changes of seven genes (i.e., *CXCL1*, *CXCL2*, *CXCL3*, *IL-6*, *MMP1*, *CCL2*, and *CCL8*) related to the senescence-associated secretory phenotype (SASP) in HDF cells with *ETS1* knockdown. Results showed that the expression of all SASP genes except one was significantly down-regulated in

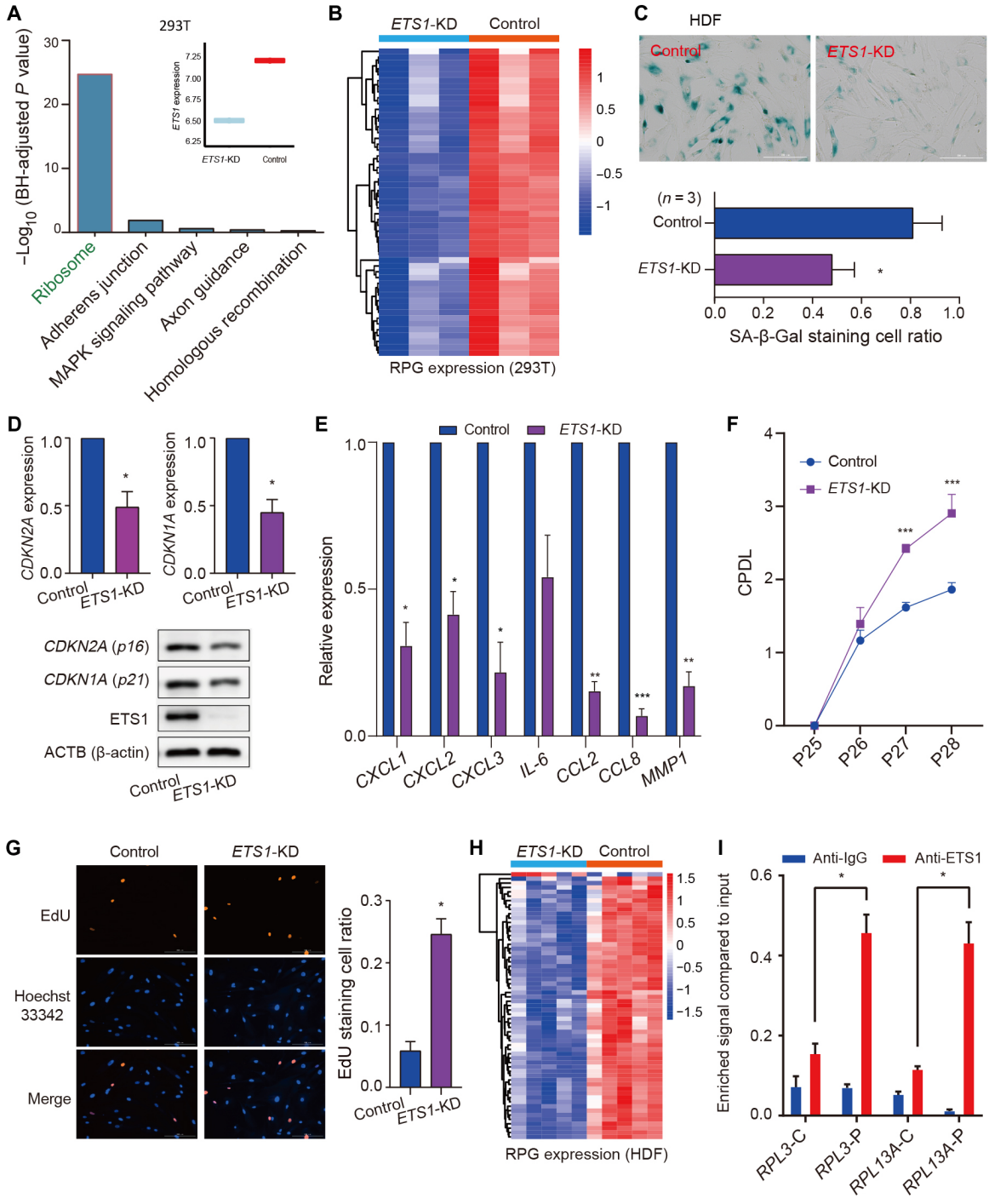

Fig. 4. Functional studies of the down-regulated *ETS1* at cellular level. (**A**) Down-regulated genes in *ETS1* knockdown (*ETS1*-KD) 293T cells were significantly enriched in ribosome pathway. MAPK, mitogen-activated protein kinase. (**B**) Heatmap for down-regulated RPGs in *ETS1* knockdown 293T cells. (**C**) Senescence-associated galactosidase beta 1 (SA-β-Gal) staining cells ratio in HDF cells. Typical images are shown on top and SA-β-Gal staining cell ratio is shown on bottom. Data are presented as means ± SEM. $n = 3$ biological replicates. (**D**) RT-qPCR for the expression levels of *CDKN1A* (*p21*) and *CDKN2A* (*p16*) in HDF cells. $n = 3$ biological replicates. Data are presented as means ± SEM. Their protein levels were validated by Western blot. (**E**) The expression of SASP genes was reduced in *ETS1* knockdown HDF cells. $n = 3$ biological replicates. Data are presented as means ± SEM. (**F**) Cumulative population doubling level (CPDL) of the HDF cells. (**G**) EdU-staining cell ratio in HDF cells. $n = 3$ biological replicates. Data are presented as means ± SEM. (**H**) Heatmap plot for the 61 RPGs with significant expression differences in *ETS1* knockdown and control HDF cells. (**I**) ETS1 binding to *RPL3* and *RPL13A* gene promoters in HDF cells at passage 20 measured by ChIP-qPCR (C, control; P, positive). $n = 3$ biological replicates. Data are presented as means ± SEM. *$P < 0.05$, **$P < 0.01$, and ***$P < 0.001$.

ETS1 knockdown HDF cells (Fig. 4E). In addition, we observed that the *ETS1* knockdown HDF cells exhibited a significant increase in cumulative population doubling level (CPDL) and 5-ethynyl-2′-deoxyuridine (EdU) staining (Fig. 4, F and G). These results support the notion that *ETS1* knockdown increases the proliferative potential of HDF cells. Of note is that these results were validated in HDF cells using a second siRNA to knockdown *ETS1* (fig. S10). Furthermore, we also found that the *ETS1* knockdown IMR-90 cells exhibited a decrease in SA-β-Gal staining cell percentage, down-regulated *CDKN2A* and *CDKN1A* expression, and increased EdU-staining cell percentage (fig. S11). Overall, these results support the function of reduced *ETS1* expression in alleviating cellular senescence.

To further validate the function of *ETS1* in the direct control of RPG expression, we performed RNA-seq on *ETS1* knockdown and control HDF cells (fig. S12A). Results showed that 60 of the 61 differentially expressed RPGs were significantly down-regulated in *ETS1* knockdown HDF cells (Fig. 4H), which also displayed reduced *CDKN2A* and *CDKN1A* expression (fig. S12B). We next detected the binding of ETS1 to two randomly selected RPG promoters (i.e., *RPL3* and *RPL13A*) using ChIP followed by qPCR (ChIP-qPCR) and found that both displayed ETS1 protein binding (Fig. 4I). Moreover, we obtained and analyzed the RNA-seq data of HDF cells from young to old passages (i.e., passage 16, passage 19, passage 28, and passage 31). We found that *ETS1* and most of RPGs (65 of 75) considered here displayed no significant correlations between their expression and cellular senescence (Pearson's correlation test, $P > 0.1$), notwithstanding that evident signatures of senescence were observed in the passage 31 HDF cells, including an increase in *CDKN2A* and *CDKN1A* expression levels, significantly increased SA-β-Gal staining, and decreased EdU staining cell percentage compared to younger cells (passage 16; fig. S13). Together, these findings suggest that the reduced level of *ETS1* can alleviate senescence via decreasing RPG expression, at least at the cellular level.

DISCUSSION

To cope with the energy crisis during aging (*23*), organisms may selectively slow down or shut off some biological processes, as suggested by the hyperfunction theory and energy maintenance theory of aging (*5*, *6*, *23*), that are indispensable for growth and development but likely redundant in mid to late life. Here, we found that the ribosome pathway and related RPGs were markedly down-regulated in LLIs from two independent cohorts (i.e., LS and LG cohorts). However, a growing body of evidence has shown that decreasing RPG or ribosomal RNA (rRNA) expression can extend the life span in model organisms, such as yeast, worm, and flies (*24*–*26*). Furthermore, several LLI specifically down-regulated RPGs (e.g., *RPS6*, *RPS11*, *RPS15*, *RPS26*, *RPL4*, *RPL6*, *RPL9*, and *RPL19*) have been determined to play some roles in life span extension of model organisms (e.g., yeast and worms) (*14*, *24*). Since ribosomes are energy-consumptive organelles responsible for protein synthesis (*13*), the down-regulated RPGs' expression results in decreased activity of protein translation. Therefore, these findings indicate that the saving of energy by reducing protein synthesis may act as a conserved life span extension mechanism across various species, including humans.

Notably, we identified ETS1 as a potential key transcriptional factor that directly controls RPG transcription in LLIs from both the LS and LG cohorts. ETS1 primarily acts as a transcriptional activator and is well described in tumors, with its overexpression leading to poorer differentiation and increased invasiveness (*27*, *28*). The contribution of *ETS1* to the LLI-specific ribosomal transcription profile was supported by both bioinformatic analyses and functional assays. The promoters of down-regulated RPGs displayed over-represented binding motifs of the ETS family, including ETS1. The *ETS1* gene was down-regulated in LLIs from both longevity cohorts and was coexpressed with the majority of RPGs. In line with this, further ChIP assays showed that ETS1 could indeed bind to the RPG promoter regions, and RNA-seq data revealed that knocking down *ETS1* could lead to reduced RPG expression.

Furthermore, the *ETS1* knockdown cells (i.e., HDF and IMR-90) displayed alleviated cell senescence and reduced RPG expression, strengthening the evidence for its role in controlling aging and longevity. Consistently, recent study showed that knocking down *Pnt* (*Drosophila* homolog of *ETS1*) can extend the life span in *Drosophila* (*29*). In addition, activating *Aop* [*Drosophila* homolog of *ETV6* (ETS variant transcription factor 6)], a *Pnt* (*ETS1*) transcriptional repressor, can also robustly extend the life span in *Drosophila* (*30*, *31*). In this study, we found that the *EVT6* gene was significantly up-regulated in the LS cohort LLIs and displayed an up-regulation trend in the LG cohort LLIs (fig. S14), which likely contributed to the *ETS1* transcriptional inhibition in the LLIs. Therefore, our study revealed a role of *ETS1* in the determination of healthy aging and longevity in humans and illustrated its ribosome-inactivating function in this process.

Our study provides evidence that reducing ribosomal activity is an alternative approach to achieve healthy aging and longevity in, at least, certain female LLIs. Furthermore, our results highlight the involvement of a conserved pathway (i.e., *ETS1*-ribosome) in determining healthy aging and longevity in humans. However, since our RNA-seq results are obtained from the peripheral white blood cells, the relevance of this observation to the other cell types or the other organs awaits further investigation.

MATERIALS AND METHODS

Study individuals

A total of 271 female individuals were recruited from Hainan Province, China. Hainan has been declared as a World Longevity Island on 27 August 2014 (Xinhua) by the International Expert Committee on Population Aging and Longevity for its highest percentage of centenarians (18.75 of 100,000) in China (China NBS 2011). In our sample collection, the ages of all samples were recorded by their identification cards and further validated by a way of recalling their life events. Among them, a population of 80 LLIs and 55 F1SPs was recruited from LS prefecture in northwest Hainan (i.e., LS cohort). Another population of 105 LLIs and 31 F1SPs was recruited from LG prefecture in southeast Hainan (i.e., LG cohort). Because the parents always live with their younger son, the F1SP samples collected are at relatively young age of about 60. Cell compositions [i.e., Lymph, Neu, and Mon] of blood samples from the LS cohort were obtained through routine blood tests. Cell compositions were not determined for the LG cohort due to limited blood samples. As F1SPs have similar living conditions as the LLIs, this reduces the effects of living environments on analysis. The study involving the use of human individuals followed the Institutional Animal Care and Use Committee guidelines. All research protocols were approved by the Ethics Committee at the Kunming Institute of Zoology, Chinese Academy of Sciences. Written informed consent was obtained from each participant in the study.

RNA-seq and read alignment

In this study, 212 and 59 libraries were constructed with polyadenylate capture and rRNA depletion methods, respectively (table S1). The RNA sample preparation and sequencing protocols have been described in our previous study. All libraries were sequenced on the Illumina HiSeq platform with 150–base pair paired-end read production.

The quantity of sequencing reads was evaluated using FastQC software (www.bioinformatics.babraham.ac.uk/projects/fastqc/). Clean reads satisfying the criteria of Q20 > 90% and Q30 > 85% were aligned to the human reference genome (UCSC build hg19) with TopHat2 (v2.0.12) using Bowtie 2 (v2.1.0) (*32*, *33*).

DEG analysis

As described in our previous study (*9*), gene-level read counts were calculated using the "*summarizeOverlaps*" function in the "GenomicAlignment" R/Bioconductor package. The RefSeq protein-coding genes (hg19) with a cutoff of at least 10 reads across all samples in a cohort were used for subsequent analyses. The DESeq2 package was used to identify the DEGs between two groups (*11*). The effects of library type and cell composition were considered in the differential expression analysis of the LS cohort.

In addition, vst-transformed gene-level read counts by "*vst*" function in DESeq2 package were used to represent the expression levels of genes in each sample (*11*). The effect of different library types on the transcriptome data in the LS cohort was corrected by "*removeBatchEffect*" in the "limma" package (*34*). For the LS cohort, *F* tests were used to further determine the DEGs by comparing the regression model [*lm(Gene expression ~ 1 + Group + Lymph + Neu + Mon)*] and the null model [*lm(Gene expression ~ 1 + Lymph + Neu + Mon)*].

Similarly, age-related genes were identified using *F* tests by comparing the regression model [*lm(Gene expression ~ 1 + Age + Lymph + Neu + Mon)*] and the null model [*lm(Gene expression ~ 1 + Lymph + Neu + Mon)*] in the F1SP samples. For the LG cohort, similar analyses were performed without consideration of cell composition. A cutoff of $P < 0.05$ was considered statistically significant.

Enrichment analysis

Functional analysis was performed using "DAVID (v6.8)" to determine the enriched KEGG pathways (*35*, *36*). A BH-adjusted *P* value threshold of <0.01 was considered statistically significant. In addition, a list of 80 RPGs was obtained from the RPG Database (http://ribosome.med.miyazaki-u.ac.jp/) (*12*).

Identification of TFs

The "*findMotifs.pl*" program in "Homer" was executed to search the overrepresented TF-binding motifs of down-regulated RPGs in LLIs (*18*). Pearson correlation tests were performed to analyze the gene coexpression relationships between the TFs and RPGs through the "*cor.test*" function in the R platform, with a *P* value cutoff of <0.05.

ChIP-seq data analysis

Ets1 ChIP-seq data of primary mouse B cells were downloaded from National Center for Biotechnology Information's Gene Expression Omnibus DataSets with accession number GSE83797 (*20*). Sequencing reads were aligned to mice reference genome (UCSC build mm10) using Bowtie 2 (v2.1.0) (*33*). Then, Ets1-binding peaks were analyzed using MACS2 program, with parameters -q 0.05 --call-summits --nomodel (v2.2.6), and 11,321 Ets1-binding regions were identified from the B cells. In addition, ETS1-binding narrow peaks of GM12878 cell line were downloaded from Encyclopedia of DNA Element database (http://hgdownload.soe.ucsc.edu/goldenPath/hg19/encodeDCC/). The peaks were annotated by "*annotatePeak*" function in "ChIPseeker" R package (*37*), with the build matched refGene information. The overrepresented KEGG pathways of ETS1 target genes were analyzed using "*enrichKEGG*" function in "clusterProfiler" R package (*38*).

Cell culture

The HDF cell line was isolated from the foreskin tissue of an adult. The HDF and IMR-90 cells were cultured in Dulbecco's modified Eagle's medium-high glucose (C11995500BT, Gibco) with 10% fetal bovine serum (35-076-CV, Gibco) and 1% penicillin/streptomycin (15140-122, Gibco) in a 37°C/5% CO_2 incubator. For siRNA transfection, the HDF and IMR-90 cells were transfected with *ETS1*-specific siRNA (target sequence: GAGCTACGATAGTTGTGAT; GGAATTACTCACTGATAAA) and nontargeting negative control siRNA (RiboBio) at a final concentration of 30 nM using Lipofectamine RNAiMAX Transfection Reagent (13778, Invitrogen) according to the manufacturer's manuals. To prolong the gene silencing effect of siRNA, a second siRNA transfection was conducted at about 72 hours after transfection. For shRNA transfection, the shRNA targeting *ETS1* was cloned into pLKO.1 lentiviral vector. The lentiviruses were harvested from human embryonic kidney–293T cells and then transfected into 293T cells to suppress *ETS1* expression. Moreover, a batch of cultured HDF cells without infection at passage 16, passage 19, passage 28, and passage 31 was collected for RNA-seq.

Real-time qPCR

Total RNA samples were extracted using TRIzol reagent (Invitrogen). Reverse transcription was performed with oligo(dT) primers using the GoScriptTM reverse transcription system (A5001, Promega) according to the manufacturer's protocols. We performed RT-qPCR with gene-specific primers using the GoTaq qPCR Master Mix (A6002, Promega). The comparative cycle threshold method was applied for quantification of gene expression, and values were normalized to β-actin (ACTB). The primers used in the study are shown in table S4.

Western blot analysis

Cells were lysed with radioimmunoprecipitation assay lysis buffer with phenylmethylsulfonyl fluoride (ST506, Beyotime Institute of Biotechnology). Proteins were quantified using the BCA Protein Assay Kit (P0010, Beyotime Institute of Biotechnology). Total protein (30 μg) was loaded onto SDS–polyacrylamide gel electrophoresis gels and subsequently transferred to poly(vinylidene fluoride) membranes (162-0177, Bio-Rad). After blocking with 5% nonfat milk in PBST (phosphate-buffered saline with Tween 20), membranes were incubated with the following primary antibodies at the suggested dilutions: anti-CDKN1A/p21 (10355-1-AP, ProteinTech Group), anti-CDKN2A/p16 (10883-1-AP, ProteinTech Group), anti-ACTB (AA128, Beyotime Institute of Biotechnology), and anti-ETS1 antibody (14069S, Cell Signaling Technology). Primary antibodies were detected with horseradish peroxidase–labeled goat anti-rabbit (A0208, Beyotime Institute of Biotechnology) or anti-mouse immunoglobulin G (IgG) (H + L) (A0216, Beyotime Institute of Biotechnology) and developed with an Enhanced Chemiluminescence Detection Kit (P0018, Beyotime Institute of Biotechnology) (*39*).

SA-β-Gal staining

SA-β-Gal staining was conducted using the Senescence Cells Histochemical Staining Kit (CS0030, Sigma-Aldrich) according to the manufacturer's instructions. Cells were visualized using a Nikon Eclipse Ti inverted microscope.

CPDL analysis

For PDL analysis, the cells at each passage were counted and passaged at the same cell density. The CPDL was calculated using the equation: $PDL_{new} = PDL_{old} + \log_2(NH/NI)$, where NH is the cell number of harvests, NI is the plating cell number, PDL_{old} is PDL at the moment of seeding, and PDL_{new} is PDL at the moment of counting. The HDF cells at passage 25 without siRNA transfection were considered as PDL = 0.

Cell proliferation assay

The HDF and IMR-90 cells were seeded into 96-well plates at a density of 8×10^3 and 1×10^4, respectively. The DNA synthesis was measured using the Cell Light EdU Apollo567 In Vitro Kit (C10338-1, RiboBio) following the manufacturer's protocols. In brief, cells were labeled with 10 μM EdU for 24 hours, fixed in 4% paraformaldehyde for 30 minutes, and then stained with Apollo 567 and Hoechst 33342. The cells were imaged by Cytation 5 Cell Imaging Multi-Mode Reader (BioTek).

ChIP assay

ChIP assays were carried out using the SimpleChIP Enzymatic Chromatin IP Kit (9003, Cell Signaling Technology) according to the manufacturer's instructions. Immunoprecipitation was carried out overnight at 4°C with an anti-ETS1 antibody (14069S, Cell Signaling Technology). Normal IgG antibody was used as the control. For ChIP-qPCR, ChIP, IgG, and input DNA samples were examined using SYBR Premix Ex Taq (RR820A, Takara). ChIP enrichment was calculated by normalization with input. The primers used for ChIP-qPCR are shown in table S5.

SUPPLEMENTARY MATERIALS

Supplementary material for this article is available at https://science.org/doi/10.1126/sciadv.abf2017

View/request a protocol for this paper from *Bio-protocol*.

REFERENCES AND NOTES

1. D. A. Chistiakov, I. A. Sobenin, V. V. Revin, A. N. Orekhov, Y. V. Bobryshev, Mitochondrial aging and age-related dysfunction of mitochondria. *Biomed. Res. Int.* **2014**, 238463 (2014).
2. S. Srivastava, The mitochondrial basis of aging and age-related disorders. *Genes* **8**, 398 (2017).
3. L. Guarente, Mitochondria—A nexus for aging, calorie restriction, and sirtuins? *Cell* **132**, 171–176 (2008).
4. C. Lerner, A. Bitto, D. Pulliam, T. Nacarelli, M. Konigsberg, H. Van Remmen, C. Torres, C. Sell, Reduced mammalian target of rapamycin activity facilitates mitochondrial retrograde signaling and increases life span in normal human fibroblasts. *Aging Cell* **12**, 966–977 (2013).
5. M. V. Blagosklonny, Aging and immortality: Quasi-programmed senescence and its pharmacologic inhibition. *Cell Cycle* **5**, 2087–2102 (2006).
6. D. Gems, L. Partridge, Genetics of longevity in model organisms: Debates and paradigm shifts. *Annu. Rev. Physiol.* **75**, 621–644 (2013).
7. R. Hitt, Y. Young-Xu, M. Silver, T. Perls, Centenarians: The older you get, the healthier you have been. *Lancet* **354**, 652 (1999).
8. H. Engberg, A. Oksuzyan, B. Jeune, J. W. Vaupel, K. Christensen, Centenarians—A useful model for healthy aging? A 29-year follow-up of hospitalizations among 40 000 Danes born in 1905. *Aging Cell* **8**, 270–276 (2009).
9. F. H. Xiao, X. Q. Chen, Q. Yu, Y. Ye, Y. W. Liu, D. Yan, L. Q. Yang, G. Chen, R. Lin, L. Yang, X. Liao, W. Zhang, W. Zhang, N. L.-S. Tang, X. F. Wang, J. Zhou, W. W. Cai, Y. H. He, Q. P. Kong, Transcriptome evidence reveals enhanced autophagy-lysosomal function in centenarians. *Genome Res.* **28**, 1601–1610 (2018).
10. W. M. Passtoors, M. Beekman, J. Deelen, R. van der Breggen, A. B. Maier, B. Guigas, E. Derhovanessian, D. van Heemst, A. J. M. de Craen, D. A. Gunn, G. Pawelec, P. E. Slagboom, Gene expression analysis of mTOR pathway: Association with human longevity. *Aging Cell* **12**, 24–31 (2013).
11. M. I. Love, W. Huber, S. Anders, Moderated estimation of fold change and dispersion for RNA-seq data with DESeq2. *Genome Biol.* **15**, 550 (2014).
12. A. Nakao, M. Yoshihama, N. Kenmochi, RPG: The ribosomal protein gene database. *Nucleic Acids Res.* **32**, 168D–1170D (2004).
13. A. W. MacInnes, The role of the ribosome in the regulation of longevity and lifespan extension. *WIREs RNA* **7**, 198–212 (2016).
14. A. Chiocchetti, J. Zhou, H. Zhu, T. Karl, O. Haubenreisser, M. Rinnerthaler, G. Heeren, K. Oender, J. Bauer, H. Hintner, M. Breitenbach, L. Breitenbach-Koller, Ribosomal proteins Rpl10 and Rps6 are potent regulators of yeast replicative life span. *Exp. Gerontol.* **42**, 275–286 (2007).
15. K. Z. Pan, J. E. Palter, A. N. Rogers, A. Olsen, D. Chen, G. J. Lithgow, P. Kapahi, Inhibition of mRNA translation extends lifespan in *Caenorhabditis elegans*. *Aging Cell* **6**, 111–119 (2007).
16. M. Molenaars, G. E. Janssens, E. G. Williams, A. Jongejan, J. Lan, S. Rabot, F. Joly, P. D. Moerland, B. V. Schomakers, M. Lezzerini, Y. J. Liu, M. A. McCormick, B. K. Kennedy, M. van Weeghel, A. H. C. van Kampen, R. Aebersold, A. W. MacInnes, R. H. Houtkooper, A conserved mito-cytosolic translational balance links two longevity pathways. *Cell Metab.* **31**, 549–563.e7 (2020).
17. S. Moreira-Ramos, F. Urbina, E. Maldonado, D. A. Rojas, Transcriptional regulation of ribosomal protein genes in yeast and metazoan cells. *J. Mol. Cell Biochem.* **2**, 5 (2018).
18. S. Heinz, C. Benner, N. Spann, E. Bertolino, Y. C. Lin, P. Laslo, J. X. Cheng, C. Murre, H. Singh, C. K. Glass, Simple combinations of lineage-determining transcription factors prime cis-regulatory elements required for macrophage and B cell identities. *Mol. Cell* **38**, 576–589 (2010).
19. E. J. Márquez, C. Chung, R. Marches, R. J. Rossi, D. Nehar-Belaid, A. Eroglu, D. J. Mellert, G. A. Kuchel, J. Banchereau, D. Ucar, Sexual-dimorphism in human immune system aging. *Nat. Commun.* **11**, 751 (2020).
20. P. Saelee, A. Kearly, S. L. Nutt, L. A. Garrett-Sinha, Genome-wide identification of target genes for the key B cell transcription factor *Ets1*. *Front. Immunol.* **8**, 383 (2017).
21. B. Y. Lee, J. A. Han, J. S. Im, A. Morrone, K. Johung, E. C. Goodwin, W. J. Kleijer, D. DiMaio, E. S. Hwang, Senescence-associated β-galactosidase is lysosomal β-galactosidase. *Aging Cell* **5**, 187–195 (2006).
22. I. Ben-Porath, R. A. Weinberg, The signals and pathways activating cellular senescence. *Int. J. Biochem. Cell Biol.* **37**, 961–976 (2005).
23. W. Mair, Tipping the energy balance toward longevity. *Cell Metab.* **17**, 5–6 (2013).
24. M. Hansen, S. Taubert, D. Crawford, N. Libina, S.-J. Lee, C. Kenyon, Lifespan extension by conditions that inhibit translation in *Caenorhabditis elegans*. *Aging Cell* **6**, 95–110 (2007).
25. N. Mittal, J. C. Guimaraes, T. Gross, A. Schmidt, A. Vina-Vilaseca, D. D. Nedialkova, F. Aeschimann, S. A. Leidel, A. Spang, M. Zavolan, The Gcn4 transcription factor reduces protein synthesis capacity and extends yeast lifespan. *Nat. Commun.* **8**, 457 (2017).
26. G. Martínez Corrales, D. Filer, K. C. Wenz, A. Rogan, G. Phillips, M. Li, Y. Feseha, S. J. Broughton, N. Alic, Partial inhibition of RNA polymerase I promotes animal health and longevity. *Cell Rep.* **30**, 1661–1669.e4 (2020).
27. J. Dittmer, The role of the transcription factor *Ets1* in carcinoma. *Semin. Cancer Biol.* **35**, 20–38 (2015).
28. G. M. Sizemore, J. R. Pitarresi, S. Balakrishnan, M. C. Ostrowski, The ETS family of oncogenic transcription factors in solid tumours. *Nat. Rev. Cancer* **17**, 337–351 (2017).
29. A. J. Dobson, R. Boulton-McDonald, L. Houchou, T. Svermova, Z. Ren, J. Subrini, M. Vazquez-Prada, M. Hoti, M. Rodriguez-Lopez, R. Ibrahim, A. Gregoriou, A. Gkantiragas, J. Bähler, M. Ezcurra, N. Alic, Longevity is determined by ETS transcription factors in multiple tissues and diverse species. *PLOS Genet.* **15**, e1008212 (2019).
30. N. Alic, M. E. Giannakou, I. Papatheodorou, M. P. Hoddinott, T. D. Andrews, E. Bolukbasi, L. Partridge, Interplay of dFOXO and two ETS-family transcription factors determines lifespan in drosophila melanogaster. *PLOS Genet.* **10**, e1004619 (2014).
31. C. Slack, N. Alic, A. Foley, M. Cabecinha, M. P. Hoddinott, L. Partridge, The Ras-Erk-ETS-signaling pathway is a drug target for longevity. *Cell* **162**, 72–83 (2015).
32. D. Kim, G. Pertea, C. Trapnell, H. Pimentel, R. Kelley, S. L. Salzberg, TopHat2: Accurate alignment of transcriptomes in the presence of insertions, deletions and gene fusions. *Genome Biol.* **14**, R36 (2013).
33. B. Langmead, S. L. Salzberg, Fast gapped-read alignment with Bowtie 2. *Nat. Methods* **9**, 357–359 (2012).
34. M. E. Ritchie, B. Phipson, D. Wu, Y. Hu, C. W. Law, W. Shi, G. K. Smyth, *limma* powers differential expression analyses for RNA-sequencing and microarray studies. *Nucleic Acids Res.* **43**, e47 (2015).

35. D. W. Huang, B. T. Sherman, R. A. Lempicki, Bioinformatics enrichment tools: Paths toward the comprehensive functional analysis of large gene lists. *Nucleic Acids Res.* **37**, 1–13 (2009).
36. D. W. Huang, B. T. Sherman, R. A. Lempicki, Systematic and integrative analysis of large gene lists using DAVID bioinformatics resources. *Nat. Protoc.* **4**, 44–57 (2009).
37. G. Yu, L.-G. Wang, Q.-Y. He, ChIPseeker: An R/Bioconductor package for ChIP peak annotation, comparison and visualization. *Bioinformatics* **31**, 2382–2383 (2015).
38. G. Yu, L.-G. Wang, Y. Han, Q.-Y. He, clusterProfiler: An R Package for comparing biological themes among gene clusters. *OMICS* **16**, 284–287 (2012).
39. Q. Yu, S.-Y. Pu, H. Wu, X.-Q. Chen, J.-J. Jiang, K.-S. Gu, Y.-H. He, Q.-P. Kong, TICRR contributes to tumorigenesis through accelerating DNA replication in cancers. *Front. Oncol.* **9**, 516 (2019).

Acknowledgments

Funding: This work was supported jointly and equally by grants from the National Key R&D Program of China (nos. 2018YFC2000400 and 2018YFE0203700). Additional support was received from Key Research Program (KFZD-SW-221), Key Research Program of Frontiers Science (QYZDB-SSW-SMC020), Strategic Priority Research Program (XDPB17), Youth Innovation Promotion Association, West Light Foundation (to F.-H.X. and Q.Y.) of the Chinese Academy of Sciences, National Natural Science Foundation of China (82071595, 91749114, 81671404, 81701394, and 31460290), Yunnan Applied Basic Research Project (2017FA038, 2018FB121, 2019FB094, 202101AT070299, 202101AS070058, and 202101AS070314), Science and Technology Leading Talent Program of the Spring City (Kunming), Yunling Scholar of Yunnan Province, and National Clinical Research Center for Geriatric Disorders (Xiangya Hospital, 2021LNJJ03). **Author contributions:** Q.-P.K. supervised and designed the project. F.-H.X. and Q.-P.K. wrote the manuscript. F.-H.X. analyzed the data. Q.Y. performed the main experiments. W.-W.C., M.-X.G., D.Y., H.-T.W., X.-Q.C., L.-Q.Y., B.-Y.Y., R.L., W.Z., X.-L.Y., and L.D. collected the samples. X.-Q.C., M.-X.G., and B.-Y.Y. performed RNA extraction for RNA-seq. J.L., Z.-L.D., J.Z., K.Y., Y.Y., and Y.H. revised the manuscript. J.L. and Z.-L.D. provided the HDF cells and performed part experiments. All authors reviewed and approved the manuscript. **Competing interests:** The authors declare that they have no competing interests. **Data and materials availability:** All data needed to evaluate the conclusions in the paper are present in the paper and/or the Supplementary Materials. The RNA-seq data supporting the current study have been deposited in the Genome Sequence Archive of the BIG Data Center, Beijing Institute of Genomics (BIG), Chinese Academy of Sciences under accession number HRA000656 and are publicly accessible at https://bigd.big.ac.cn/gsa-human/.

Submitted 10 October 2020
Accepted 27 February 2022
Published 27 April 2022
10.1126/sciadv.abf2017